# FRACTAL ANALYSIS OF A VOLTAGE-DEPENDENT POTASSIUM CHANNEL FROM CULTURED MOUSE HIPPOCAMPAL NEURONS

LARRY S. LIEBOVITCH* AND J. MICHAEL SULLIVAN‡
*Department of Ophthalmology, Columbia University, College of Physicians and Surgeons, New York, New York 10032; and ‡Departments of Physiology-Biophysics and Anesthesiology, Mt. Sinai School of Medicine, New York, New York 10029

ABSTRACT The kinetics of ion channels have been widely modeled as a Markov process. In these models it is assumed that the channel protein has a small number of discrete conformational states and the kinetic rate constants connecting these states are constant. In the alternative fractal model the spontaneous fluctuations of the channel protein at many different time scales are represented by a kinetic rate constant $k = At^{1-D}$, where $A$ is the kinetic setpoint and $D$ the fractal dimension. Single-channel currents were recorded at 146 mM external $K^+$ from an inwardly rectifying, 120 pS, $K^+$ selective, voltage-sensitive channel in cultured mouse hippocampal neurons. The kinetics of these channels were found to be statistically self-similar at different time scales as predicted by the fractal model. The fractal dimensions were ~2 for the closed times and ~1 for the open times and did not depend on voltage. For both the open and closed times the logarithm of the kinetic setpoint was found to be proportional to the applied voltage, which indicates that the gating of this channel involves the net inward movement of approximately one negative charge when this channel opens. Thus, the open and closed times and the voltage dependence of the gating of this channel are well described by the fractal model.

## INTRODUCTION

Ions can cross the hydrophobic cell membrane through the hydrophilic interior of ion channels. Everpresent thermal fluctuations provide the energy for these channels to spontaneously change their conformation so that they are continuously fluctuating between open and closed states. The patch clamp technique can resolve the open and closed durations of an individual channel by measuring the picoamp currents across a small membrane patch with a few such channels (1, 2). Thus, the sequence and duration of the conformational states of the channel are obtained. This provides a unique opportunity to study the kinetics of the spontaneous conformational changes of a single molecule at a time.

The kinetics of these channels have been widely modeled, and experimental results from single channel and noise analysis experiments interpreted, by assuming that the channel has a small number of discrete conformational states, such as closed $\rightleftharpoons$ closed $\rightleftharpoons$ open, and that the transition probabilities between these states can be described by a Markov process (1–14). That is, it is assumed that the transition probabilities per unit time, the kinetic rate constants, are independent of the time spent in the current state and also independent of the history of the previous sequence of states of the channel. However, these assumptions may not be consistent with the physical chemistry of the dynamics of the conformational changes in proteins. Many proteins have large numbers of conformational states that are separated by only small energy barriers. Moreover, changes in protein conformation occur over many time scales from picosecond rotations around bonds to unfolding modes that last minutes (15–23). Thus, a channel would be expected to have a continuum of many conformational states, rather than a few discrete states, and have dynamic processes and thus "memory" at all time scales.

A new model of channel kinetics, consistent with these ideas, has recently been proposed (24–26). In the fractal model, the closed and open states are each represented as a continuum of many conformational states. The kinetic rate constant for leaving the closed or open states is then a mixture of the rate constants for leaving this collection of states. The fractal model proposed that this effective rate constant has the form $At^{1-D}$, where $A$ is the kinetic setpoint, $t$ is the time the channel has resided in the current state, and $D$ is the fractal dimension. This form was chosen because many other physical systems composed of processes that occur over a large range of spatial or temporal scales display this type of scaling.

We will first review the fractal model and then use it to analyze and interpret the single channel currents recorded from a $K^+$-selective channel in cultured mouse hippocampal pyramidal cells. This is a large conductance inward

rectifying channel. Its activity is voltage dependent in that the fractional time it remains open decreases as the cell is hyperpolarized. Channels of this type were studied by Wong and Clark (27) and later by Sullivan and Cohen (28), Huguenard and Alger (29), and Sullivan (30, 31).

## FRACTAL MODEL OF ION CHANNEL KINETICS

Building on a long history of mathematical ideas, Mandelbrot developed, organized, and expanded the concept he named "fractals" (32–40). A fractal object has a similar appearance when viewed at different scales of magnification. This property of fractals is called statistical self-similarity. For example, the coast of Britain looks just as "wiggly" on maps of different scales (40). Although the wiggles are of similar size when measured in centimeters on the map, they will correspond to different lengths in kilometers because the maps have different scales of centimeters to kilometers.

The total length of the coast depends on the scale of the map on which it is measured. As the measurement is done on maps of finer scale, the irregularities resolved will be finer, so that the length measured in kilometers is therefore longer. For coastlines and many other objects the value $L$ measured for a property is proportional to a power of the scale $\epsilon$ at which it is measured, namely that $L = A\epsilon^{D_T - D}$, where $A$ is a constant, $D_T$ is the topological dimension, and $D$ is the fractal dimension. This scaling relationship is an important property of fractals. For the west coast of Britain where $D_T = 1$, Richardson (41) found that the fractal dimension $D = 1.25$. These intuitive notions of self-similarity and scaling are both contained in the formal definition that a set in a metric space is fractal if the Hausdorff-Besicovitch dimension exceeds the topological dimension (33, p. 361).

In the last few years there has been an explosive growth in the objects and processes that have been found to have fractal properties. For example a small sampling of fractals found in nature include: the perimeters of clouds (42); the surface area of proteins (43); the surface area within bulk samples of minerals (44); the surface areas of the membranes of intracellular organelles (45); Brownian motion (33, 46); the intensity of earthquakes (47); the branching pattern of the bronchial tree (48); the patterns formed when water is injected into clay (49, 50), or lipids into lipids (51), or the pathway of sparks in dielectric breakdown (50); the motions induced by photodissociation of CO-myoglobin (52); the shape of soot particles (53); the vibrations in solid state materials (54); and the dielectric relaxation of glasses and polymers (55–57).

To formulate a channel model where the kinetics have the fractal properties discussed above we describe the channel as having one open and one closed state,

$$\text{closed} \underset{k_c}{\overset{k_o}{\rightleftharpoons}} \text{open},$$

where the kinetic rate constants $k_o(t)$ and $k_c(t)$ are the probabilities per unit time of leaving the closed and open states. We will derive the properties of the closed state. The equations for the open state are analogous with $k_o(t)$ replaced by $k_c(t)$. Let $P(t)$ be the probability that the channel remains closed over the interval $[0, t]$. The probability that the channel remains closed over the interval $[0, t + \Delta t]$ is then equal to the probability that the channel is closed up to time $t$ and that it does not open in the next $\Delta t$ interval. Taking the limit $\Delta t \to 0$ and integrating yields the result (see for example reference 26) that

$$\int \frac{dP(t)}{P(t)} = -\int k_o(t)\, dt. \tag{1}$$

The probability per unit time that the channel is closed for duration $t$ is given by the probability density function

$$f(t) = -\frac{dP(t)}{dt}. \tag{2}$$

For a channel with fractal kinetics, the faster we look, the faster the channel will flicker open and closed. Just as the coast of Britain is longer when we measure it at finer spatial resolution, the effect kinetic rate constant of the channel is larger when we measure it at finer temporal resolution. Let the smallest time interval that we can resolve define the effective time scale $t_{eff}$. We can only detect channel closings of duration $t > t_{eff}$. Thus, the meaningful measurement of channel kinetics is not the kinetic rate constant, which is the probability that a closed channel will open; but rather the effective kinetic rate constant, $k_{eff}$, which is the conditional probability that a channel that has been closed for at least duration $t_{eff}$ will open.

Let $\mathcal{A}$ be the probability that a closed channel will open at time $T$ in the interval $t_{eff} < T \le t_{eff} + \Delta t$ and $\mathcal{B}$ the probability that the channel will remain closed for at least duration $T > t_{eff}$. The effective kinetic rate constant $k_{eff}$ evaluated at $t_{eff}$ is thus probability per unit time for event $\mathcal{A}$ given that event $\mathcal{B}$ has already occurred, namely $k_{eff} = \lim_{\Delta t \to 0} \text{prob}(\mathcal{A}|\mathcal{B})/\Delta t$. The definition of the conditional probability is that prob $(\mathcal{A}|\mathcal{B}) = \text{prob}(\mathcal{A} \text{ and } \mathcal{B})/\text{prob}(\mathcal{B})$. Note that $\mathcal{A} \cap \mathcal{B} = \mathcal{A}$, that is, the event $t_{eff} < T \le t_{eff} + \Delta t$ and the event $t_{eff} < T$, is the same as the event $t_{eff} < T \le t_{eff} + \Delta t$. Hence prob $(\mathcal{A} \text{ and } \mathcal{B}) = \text{prob}(\mathcal{A})$. Thus, we find that

$$k_{eff}(t_{eff}) = \frac{f(t_{eff})}{P(t_{eff})} = -\left.\frac{d[\ln P(t)]}{dt}\right|_{t = t_{eff}}. \tag{3}$$

In renewal theory $k_{eff}$ is called the "age-specific failure rate" and it gives the conditional probability that a component (e.g., a light bulb) that has survived to age $t_{eff}$ will fail in the next $\Delta t$ interval. The derivation of $k_{eff}$ given above is from the monograph on renewal theory by Cox (58, pp. 3–5). The function $k_{eff}$ is also widely used in actuarial

work, for example, in determining premiums for life insurance policies.

To formulate a model of ion channel kinetics having fractal properties we assume that the effective kinetic rate constant for leaving the continuum of protein conformations that constitute the closed state is given by

$$k_{\text{eff}}(t_{\text{eff}}) = A\, t_{\text{eff}}^{1-D}. \tag{4}$$

This effective kinetic rate constant summarizes the information about the processes that happen at many different time scales. The fractal dimension $D$ determines how sensitive $k_{\text{eff}}$ is to changes in temporal scale. The kinetic setpoint $A$ determines if all the processes happen slowly or rapidly. Note that since the current through the channel depends only on a single variable, that is time, the topological dimension $D_T = 1$.

The definition of the effective rate constant (Eq. 3) and the fact that it satisfies a fractal scaling relationship (Eq. 4) requires that the microscopic kinetic rate constant $k_o(t)$ is given by

$$k_o(t) = At^{1-D}. \tag{5}$$

Note that $t$ is the time the channel has spent in its current state and $k_o$ is the transition probability per unit time out of that state. When $D > 1$, the longer the channel resides in any state, the less likely it is to exit that state in subsequent time intervals.

The kinetic rate constant $k_o(t)$ from Eq. 5 can be substituted into Eq. 1 to find that

$$P(t) = e^{-[A/(2-D)]t^{2-D}} \tag{6}$$

This form is known as the Weibull distribution (58, pp. 20–22). Since it was first used by Kohlrausch in 1864 to describe mechanical creep it has been used to model many different physical processes (57). In the study of the dielectric relaxation of glasses and polymers it is known as the stretched exponential or Williams-Watts law (55–57). From Eqs. 2 and 6 we find that the frequency histogram of closed times is given by

$$f(t) = A\, t^{1-D} e^{-[A/(2-D)]t^{2-D}} \tag{7}$$

The rate of channel openings and closings should depend inversely on the time scale, so that $D \geq 1$. To normalize the probability distribution requires that $\lim_{t\to 0} P(t)$ exist, which is true only if $D < 2$. Thus, the fractal dimension $D$ is restricted to the range $1 \leq D < 2$. (Actually, this upper bound is only a weak restriction because the probability distribution can be renormalized using the number of observed closed durations rather than the total number of closed durations when $D \geq 2$.)

## METHODS

### Experimental Techniques

Mouse embryonic hippocampal neurons (14–16 d gestation) were maintained in primary dissociated culture according to established protocols (59). Briefly, embryonic mouse hippocampi from Swiss Webster mice (Buckberg Laboratory Animals, Tompkins Grove, NY) were isolated and cut into small clumps in dissecting solution (Eagle's minimum essential medium [MEM-GG] supplemented with 6 g/liter glucose, 2 mM L-glutamine, and 15 mM Hepes), and treated with trypsin (100 μg/ml for 20 min at 35°C under 5% $CO_2$/95% air [vol/vol]. After pelleting of tissue and resuspension in MEM-GG supplemented with 5% (vol/vol) fetal bovine serum (FBS) and 5% (vol/vol) horse serum (HS)(MEM-GG-BH), the suspension was triturated four times with a 25-gauge needle on a 5-ml syringe and plated on 18-mm collagen-coated (60) or poly-L-lysine (61, 62) coverslips (Carolina Biological Supply Co., Burlington, NC) in 35- or 60-mm Falcon culture dishes (Becton, Dickinson & Co., Oxnard, CA) on a drop of MEM-GG-BH. About 1/4 to 1/2 hippocampus was plated per coverslip overnight under 5% $CO_2$/95% air (vol/vol) at 35°C. The next day 1.5 ml of MEM-GG-BH was added or coverslips were transferred to dishes where whole brain cultures (minus hippocampus) had been grown over the previous 7–9 d in MEM-GG supplemented with 20% FBS and 2% HS. At the time of transfer to whole brain co-culture, serum-containing medium was totally replaced with a serum-free chemically defined medium (63–65) consisting of MEM-GG supplemented with insulin (5 μg/ml), human transferrin (100 μg/ml), sodium selenite (30 nM), triiodothyronine (0.3 nM), hydrocortisone (20 nM), and progesterone (20 nM). All cultures were maintained at 5% $CO_2$/95% air (vol/vol) at 35°C and media was changed weekly for both serum-containing and "serum-free" cultures. All media formulations, sera, and L-glutamine were obtained from Gibco (Grand Island, NY). All hormones and supplements were obtained from Sigma Chemical Co. (St. Louis, MO) except dextrose (Fisher Scientific Co., Pittsburgh, PA). Pyramidal cells maintained in serum-containing or serum-free medium had similar shapes with well developed dendritic arborizations after a few days in culture. Hippocampal pyramidal cells used for electrophysiological analysis had been maintained in cultures for 4 d to longer than 2 wk and were selected solely on the basis of morphological criteria (31).

Coverslips containing pyramidally shaped neurons were washed two to three times in the extracellular electrophysiological recording solution containing (in mM): 145 NaCl, 5.6 KCl, 1.0 $CaCl_2$, 0.8 $MgCl_2$, 5.6 glucose, and 4.0 Hepes-KOH, pH 7.2. Coverslips were then transferred to a specially designed chamber and viewed under 400× Nomarski (Diaphot) optics (Nikon Inc., Garden City, NY).

Patch electrodes were fabricated from Corning 7052 glass (Garner Glass Co., Clairmont, CA) according to the method of Corey and Stevens (66) and coated with Sylgard 184 elastomer (Dow Corning Corp., Midland, MI) to within 100 μm of the tip, and firepolished to resistances of 5–10 MΩ when filled with cell-attatched patch recording fluids. Electrodes were secured in a specially designed holder (EW Wright, Guilford, CT) which was plugged directly into the headstage BNC. Patch clamp recording was used according to the method of Hamill et al. (9) using a Dagan 8900 Patch-Whole-Cell Clamp with a selected low noise 10 GΩ headstage (Dagan Corp., Minneapolis, MN; headstage 8930A). The ground and pipette electrodes were Ag/AgCl junctions. Electrode tips were initially filled by suction and finally filled to about a 1-cm column of fluid by backfilling with fine polystyrene needles attached to a syringe with a 0.22-μm filter (No. 4192; Gelman Sciences, Inc., Ann Arbor, MI). The experiments reported here were done with a pipette filling solution containing (in mM): 145.6 KCl, 1.0 $CaCl_2$, 1.0 $MgCl_2$, and 4.0 Hepes-KOH, pH 7.2. Electrodes were placed onto the surface of the cultured hippocampal neuron cell bodies (Leitz manipulators) and positioned until a slight dimpling of the surface was noted under 400× Nomarski. Slight suction (10–20 cm water) was applied to the pipette interior to obtain gigaohm seals while constantly adjusting the junction potential and was followed by electronic subtraction of pipette/patch input capacitance using a three time constant correction circuit.

Using conditions employed previously to identify single, inward rectifying $K^+$ channels in nonneuronal preparations (67–70) or in hippocampal neurons (27) with high concentrations of $K^+$ in the pipette it was often possible (~10–20% of patches) under conditions of stable, gigaohm seals to identify a high conductance, $K^+$ selective channel with inward rectify-

ing I-V curves (28, 30, 31). Detailed analysis of the conductance properties of these channels indicates apparent ideal selectivity for $K^+$ permeation, a square root dependence of extracellular $K^+$ on conductance, apparent block by $Cs^+$and $Ba^{2+}$, and saturation of inward current with increasing $K^+$ at constant voltage in apparent violation of the Goldman-Hodgkin-Katz equation (31). In addition these channels also exhibit submaximal current levels, which have properties consistent with subconductance states (28, 30, 31).

Single channel currents from cell attached patches with command potentials at hyperpolarizing voltages of 0, 22, 41, and 60 mV (relative to the resting membrane potential) were recorded on FM tape (model B, 4 track tape recorder; A. R. Vetter Co., Rebersburg, PA) at 7½ in./s (~2.25 kHz). Single channel open and closed times were measured in two ways: )(*a*) by playback of tape records at ⅛ recording speed (15/16 ips) onto a paper recorder (frequency response ~100 Hz; Gould Inc., Cleveland, OH) and then manual measurement of the duration of events, or (*b*) digitization of analog data from tape at 10 kHz on a Data General Eclipse System (Westboro, MA) and analysis using the IPROC automated pattern recognition program (71) employing half-maximal current amplitude event detection criterion and a pattern recognition algorithm for noise rejection (72, 73).

## Markov Analysis

Open and closed time duration histograms were fitted to single and multiple exponential functions using a Marquardt-Levinberg algorithm (74) that does not require analytical derivatives and incorporates subroutine ZXSSQ by International Mathematical and Statistical Libraries Inc. (Houston, TX). The open time distributions could always be fit by a single exponential while triple exponentials were necessary to fit the closed time distributions. These distributions were interpreted in terms of a

$$\text{closed} \underset{k_{21}}{\overset{k_{12}}{\rightleftharpoons}} \text{closed} \underset{k_{32}}{\overset{k_{23}}{\rightleftharpoons}} \text{closed} \underset{k_{O3}}{\overset{k_{34}}{\rightleftharpoons}} \text{open}$$

kinetic model. This model was chosen because of its relative simplicity and because of its useful application to other $K^+$ channels (75). The rate constant $k_{O3}$ is equal to the inverse of the time constant of the open time distribution. The other rate constants were calculated by solving the nonlinear equations (3.65, 3.66, 3.67, and 3.70) of Colquhoun and Hawkes (11) with the time constants and amplitudes of the total closed distribution function as input. A program called 4STATE (incorporating IMSL subroutine ZSPOW) was used to solve the system of nonlinear algebraic equations at each voltage in each patch.

## Fractal Analysis

Liebovitch et al. have shown that a plot of log $k_{eff}$ vs. log $t_{eff}$ is a sensitive method to analyze ion channel kinetics (24–26). If there are multiple plateaus on this plot, then the channel has multiple, discrete states that can be well represented by a Markov process. However, if the kinetics of the channel are fractal, then this plot will be a straight line of the form log $k_{eff} = (1 - D) \log t_{eff} + \log A$. Thus, the two parameters of the fractal model, the fractal dimension $D$ and the kinetic setpoint $A$, can be determined from the slope and intercept of this plot.

The analytic definition $k_{eff}$ (Eq. 3) can be recast into a form more useful for analyzing the experimentally measured closed durations. For a two-state closed ⇌ open Markov process, that is, the fractal model with $D = 1$, then $P(t) = \exp(-k_o t)$, $f(t) = k_o \exp(-k_o t)$, and $k_o = -\mathrm{d}/\mathrm{d}t[\ln P(t)]$ where $k_o$ is a constant. Note the similarity of this form for $k_o$ to that for the effective kinetic rate constant $k_{eff} = -\mathrm{d}/\mathrm{d}t[\ln P(t)]|t = t_{eff}$. Thus, over a small range of times the kinetics of any channel are locally of the form of a closed ⇌ open Markov process with $k_{eff} = k_o$.

Thus, $k_{eff}$ is equal to minus the slope of $\ln f(t)$ vs. $t$ evaluated over a small range of closed durations. To do this, we construct frequency histograms of closed times each with a different bin size. The bin size $t_b$ determines the effective time scale of the analysis and thus $t_b = t_{eff}$. Then, for each histogram, we use least squares to determine the slope over the second through fourth bins. We must exclude the first time bin that includes the closings $t \ll t_b$ that are much less than the time scale $t_b$, and the longer time bins that include all the closings $t \gg t_b$ that are much longer than the time scale $t_b$. This procedure thus determines $k_{eff}$ as a function of $t_{eff}$. We have previously validated this procedure by comparing $k_{eff}$ determined analytically from fractal and multistate Markov models using Eq. 3 with $k_{eff}$ determined by constructing the closed time histograms from finite difference simulations of single channel currents from those same models (26). The effective kinetic rate constants determined by both methods were very similar. However, for the channel models with fractal kinetics, the plots of log $k_{eff}$ vs. log $t_{eff}$ based on this fitting procedure overestimated the fractal dimension $D$ by ~10%.

Once the fractal dimension $D$ and the kinetic setpoint $A$ have been determined from the plot of log $k_{eff}$ vs. log $t_{eff}$ it is simple to fit the fractal model to the experimentally measured distribution of closed times. The number of closings of duration $t$ to $t + \Delta t$ is given by $N(t) = N_T \Delta t f(t)$. Since $f(t)$ depends only on $D$ and $A$ it is already completely known. To determine $N_T$ we minimize the residuals $S = \Sigma_{i=1,n}[\ln [N_T f(t_i)] - \ln [N(t_i)/\Delta t]]^2$, where $n$ closed durations were observed. We use the logarithms because for the limiting case $D = 1$ this reduces to a semilogarithmic fit, which can be done analytically and because $f(t)$ often extends over several decades so that if the logarithms are not used then only the few highest values of $f(t)$ would actually influence the fitting procedure. Minimizing the residuals, $\partial S/\partial N_T = 0$, we find that $N_T = \exp\{(-1/n)\Sigma_{i=1,n} \ln [f(t_i)\Delta t/N(t_i)]\}$.

A Macintosh microcomputer (Apple Computer Inc., Cupertino, CA) was used for the data analysis. The open and closed times were stored in a spreadsheet (Microsoft Excel), the mathematics performed by programs in Microsoft BASIC, and the results plotted with Cricket Graph. Using Switcher to load several programs in memory at once it is very easy to transfer data and results between programs by using the buffer (the clipboard) which can be accessed by all programs on the Macintosh.

Note that this fractal analysis uses only a least squares fit of a straight line which can be done analytically to determine $D$ and $A$ and a sum to determine $N_T$. These are closed (and not iterated) procedures and considerably simpler than the much more complex and often numerically delicate techniques required to determine the kinetic rate constants of the multiple state Markov models.

# RESULTS

## Markov Model

At least one open and three closed states were required to fit the distributions of open and closed durations. The details of the fitting procedure and the results are described by Sullivan (31) and Sullivan and Cohen (manuscript in preparation). A very complex picture emerges of the voltage dependence of this channel. The variation of the time constants for leaving the open and closed states are shown in Fig. 1. The time constant from the open state decreases with hyperpolarization while for the closed states, the short time constant remains approximately constant, the medium time constant decreases, and the long time constant increases with hyperpolarization. As shown in Fig. 2 the kinetic rate constants of this Markov model show no consistent changes that can be interpreted in a simple clear physical model.

Markov models cannot be uniquely determined from just the distributions of the open and closed durations. Thus, it is possible that another Markov model (that we were unable to find) might prove easier to interpret in

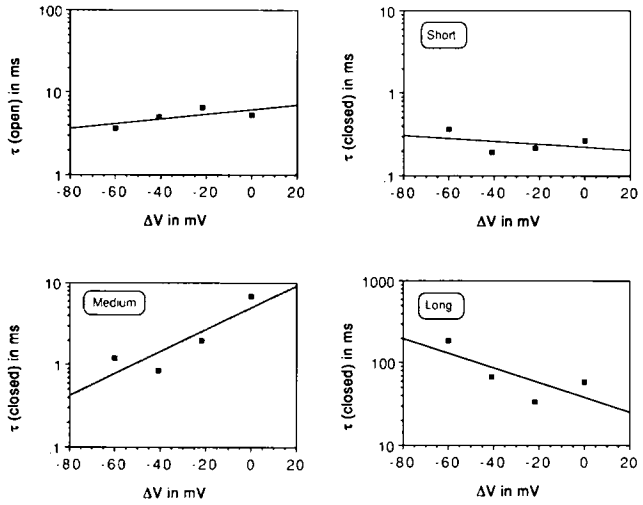


FIGURE 1 The open times could be fit by a single exponential and the closed times by the sums of three exponentials. The variation of those time constants with voltage is shown above. The data shown here are the average from two patches.

terms of a physical model. It is also possible that the data here are insufficient to produce good estimates of all the parameters that a multi-state Markov model requires. However, the data were sufficient to produce good estimates of the fractal parameters.

## Fractal Model

The open and closed durations measured from the single channel records were used to construct histograms of bin sizes 1, 2, 4, 8, 16, 32, 64, 128, 256, and 512 ms. Only histograms with enough statistical accuracy to have monotonically decreasing nonzero numbers of durations in the first four bins were used for further analysis. A sample of these histograms, when 0 mV was applied, is shown in Figs.

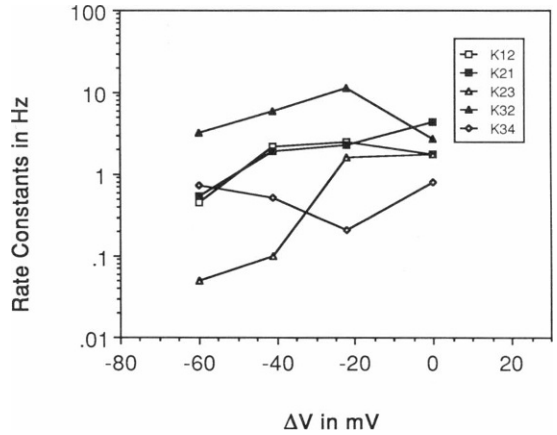


FIGURE 2 The variation of the kinetic rate constants with voltage calculated from the Markov model

$$\text{closed} \underset{k_{21}}{\overset{k_{12}}{\rightleftharpoons}} \text{closed} \underset{k_{32}}{\overset{k_{23}}{\rightleftharpoons}} \text{closed} \underset{k_{O3}}{\overset{k_{34}}{\rightleftharpoons}} \text{open.}$$

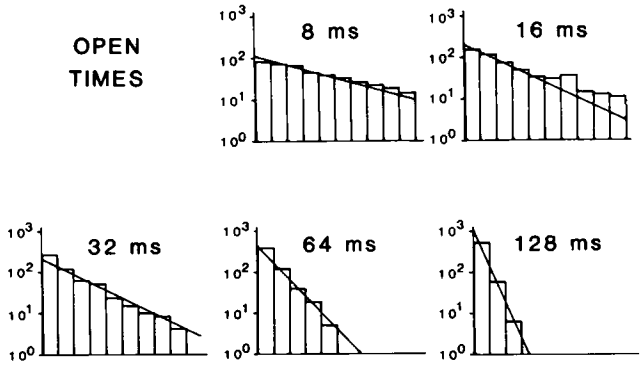


FIGURE 3 The open times recorded at 0 mV were used to construct frequency histograms of bin width 8, 16, 32, 64, and 128 ms. The lines are the least squares fit of a single exponential using the second through fourth bins. The negative of the slopes of these lines equals the effective kinetic rate constant $k_{eff}$ for leaving the open state at the effective time scale $t_{eff}$ equal to the bin size.

3–4. The lines on these figures are a least squares fit using the second through fourth bins.The negative values of the slopes of these lines are the effective rate constants $k_{eff}$ shown in Fig. 5. These plots of log $k_{eff}$ vs. log $t_{eff}$ for both the open and closed times do not have the plateaus that would indicate the existence of the multiple discrete states predicted by the Markov models. Rather, they are approximately straight lines, indicating that these channels can be represented by a model with fractal kinetics.

As shown in Fig. 6, the fractal dimension $D$ for both the open and closed times does not vary with the applied voltage. We found that $D$(open) = 1.34 ± 0.11 (mean ± SEM) and that $D$(closed) = 2.07 ± 0.12. The fractal model of ion channel kinetics predicts that the fractal dimension $D$ should be within the range $1 \leq D < 2$. The values found for $D$(open) and $D$(closed) are within this range. The value of $D$(open) is greater than one ($t$ test, $P < 0.025$) and the value for $D$(closed) is not greater than two ($t$ test, $P < 0.3$). Because the fitting procedure tends to overestimate the fractal dimension by ~10%, we believe

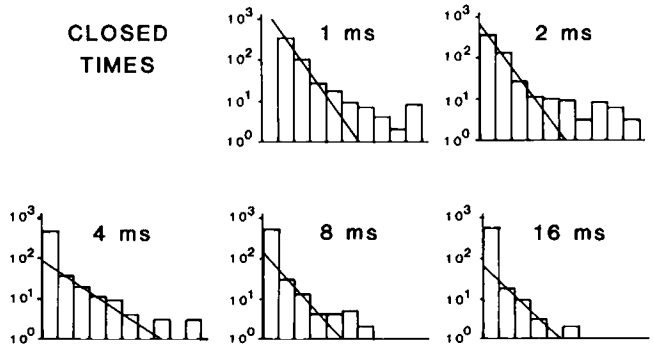


FIGURE 4 The closed times recorded at 0 mV were used to construct frequency histograms of bin width 1, 2, 4, 8, and 16 ms. The lines are the least squares fit of a single exponential using the second through fourth bins. The negative of the slopes of these lines equals the effective kinetic rate constant $k_{eff}$ for leaving the closed state at the effective time scale $t_{eff}$ equal to the bin size.

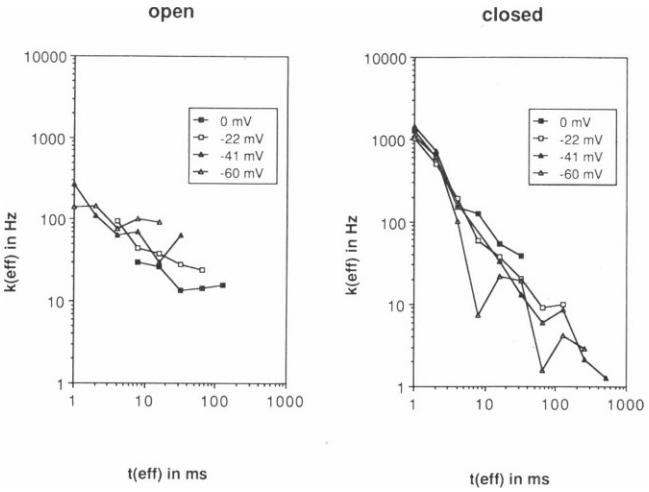


FIGURE 5 The effective kinetic rate constants $k_{eff}$ for leaving the open and closed states are plotted versus the effective time scale $t_{eff}$ for patches that were voltage clamped at hyperpolarizing voltages of 0, 22, 41, and 60 mV. There are no plateaus in the plot that would indicate the existence of multiple, discrete conformational states predicted by the Markov models of ion channel kinetics. The linearity of the data at each voltage is consistent with the fractal model of ion channel kinetics. The slope and intercept of the lines on these plots determines the fractal dimension $D$ and the kinetic setpoint $A$.

that $D$(open) $\approx 1$ and $D$(closed) $\approx 2$. The kinetic setpoint $A$ was strongly dependent on voltage. As also shown in Fig. 6, -log[$A$(open)] and log[$A$(closed)] are proportional to voltage with approximately the same constant of proportionality.

When $D \approx 1$, the probability density function $f(t) = A\exp(-At)$. Hence, $D$(open) $\approx 1$ implies that the histogram of open times should be well fit by a single exponential. Thus, on a semilogarithmic plot the open times should

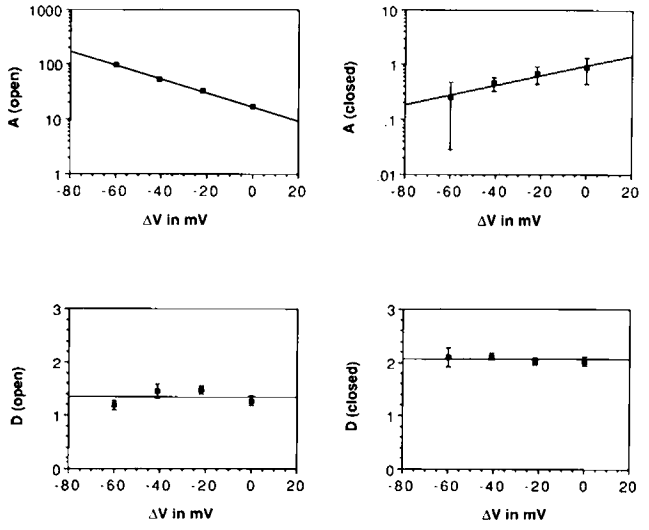


FIGURE 6 The dependence of the kinetic setpoint and fractal dimension on voltage are shown. The fractal dimension does not depend on voltage. The logarithms of the kinetic setpoint for the open and closed times are proportional to voltage with approximately the same constant of proportionality.

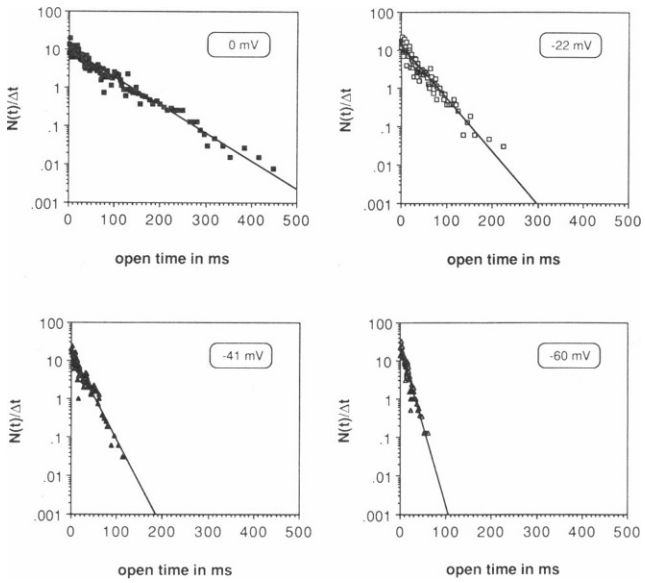


FIGURE 7 Semilogarithmic plot of the open time histograms. The lines are the best fit of a single exponential to the data.

be well fit by a straight line and this is indeed true as seen in Fig. 7. The closed times, also presented on semilogarithmic plot in Fig. 8, are also well represented by the fractal model.

When $D \approx 2$, then $t^{2-D} = e^{(2-D)\ln t} \approx 1 + (2 - D)\ln t$, thus the probability density function $f(t) \approx A\exp\{-[A/(2 - D)]\}t^{1-D-A}$. That is, when $D \approx 2$, the frequency histogram of the fractal model is no longer a stretched exponential, but becomes a power law where $f(t) \propto t^{1-D-A}$. Hence, $D$(closed) $\approx 2$ implies that the histogram of closed times should be well fit by a straight line on a log-log plot. This is indeed the case as shown in Fig. 10. For comparison a log-log plot of the open times is shown in Fig. 9. Since

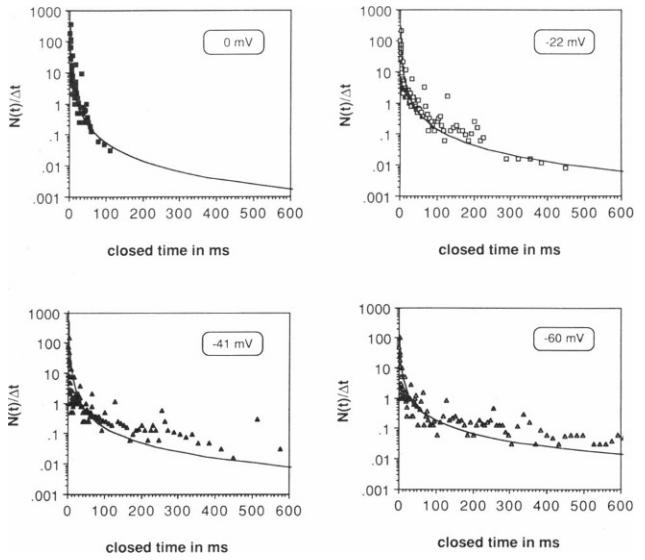


FIGURE 8 Semilogarithmic plot of the closed time histograms. The lines are the best fit of the fractal model to the data.

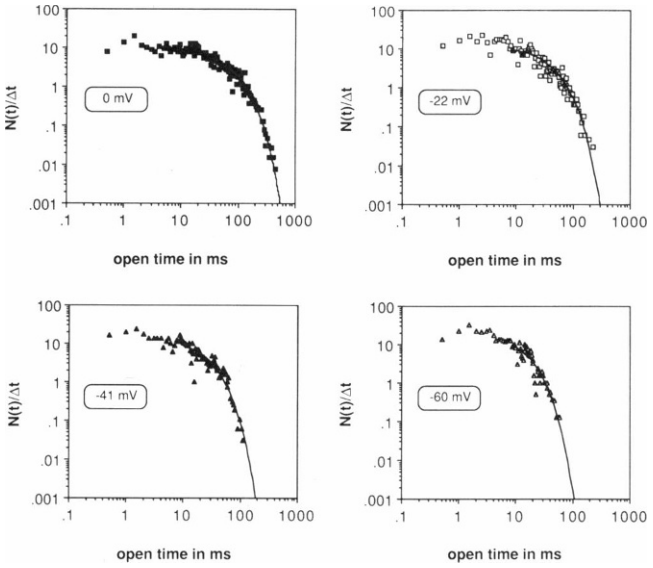


FIGURE 9 Logarithmic-logarithmic plot of the open time histograms. The lines are the best fit of a single exponential to the data.

$D$(open) is not close to 2, the open times are not a straight line on a log-log plot.

## DISCUSSION

Ion channels open and close spontaneously. The mathematical model known as a Markov process, which has been widely used to represent the kinetics of these channels and interpret the results from single channel and noise analysis experiments, assumes that the channel proteins have only a few discrete conformational states. However, it is known that the spontaneous fluctuations in the conformation of proteins involve many different processes that occur over many different time scales from $10^{-15}$ to $10^{3}$ s (15–23). This suggests that the fluctuations of the channel protein pass through a very large number of conformational states. To reflect this behavior Liebovitch et al. (24–26) proposed a new model of ion channel kinetics where the channel is represented by a continuum of many conformational states. In this fractal model the dynamic processes that take place over many different time scales are represented by a kinetic rate constant that has the fractal form $k = At^{1-D}$. This form was chosen because many other systems (from the length of the coast of Britain to dielectric relaxation in glasses) that are composed of processes that occur over a large range of spatial or temporal scales have this type of scaling behavior (32–57). The fractal dimension $D$ determines the relative contribution of processes at different time scales and the kinetic setpoint $A$ determines if all the processes happen slowly or rapidly.

We used both the Markov and fractal models to interpret single channel currents recorded from a $K^+$-selective, voltage-dependent channel in cultured neurons from the mouse hippocampus. The histograms of the durations of the open and closed times are well fit by both models. The fractal model is more parsimonious about its assumptions than the Markov model. The fractal model depends on four parameters while the Markov closed ⇌ closed ⇌ closed ⇌ open model depends on six kinetic rate constants. Also, the mathematical analysis needed to determine the parameters of the fractal model is much simpler than that required to determine the parameters of the Markov model.

The voltage dependence of the kinetic rate constants of the Markov model is complex. Each of the many kinetic rate constants are independent parameters having a unique and independent variation with voltage. However, in the fractal model, it is seen that the entire voltage dependence of all the short, medium, and long closed and open times of the channel can be understood entirely in terms of how the kinetic setpoint, varies with voltage. As seen in Fig. 6 the fractal dimensions of both the open and closed states does not depend on voltage. However, $-\log[A(\text{open})]$ and $\log[A(\text{closed})]$ are proportional to voltage with approximately the same constant of proportionality. This suggests

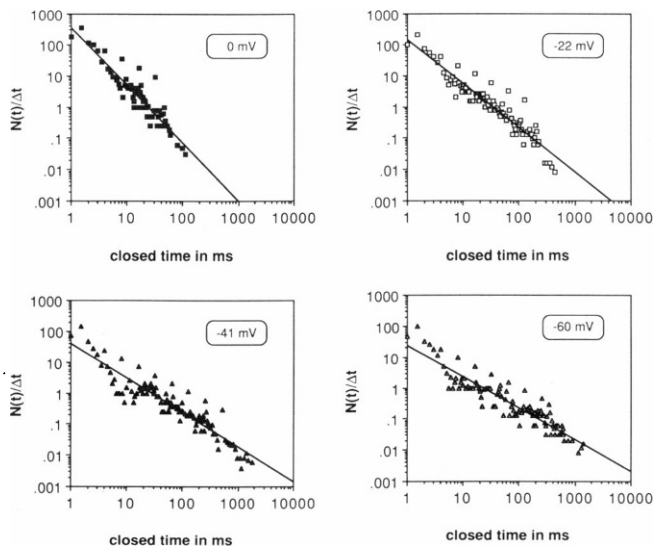


FIGURE 10. Logarithmic-logarithmic plot of the closed time histograms. As determined from the plot of log $k_{\text{eff}}$ vs. log $t_{\text{eff}}$ in Fig. 5, $D$(closed) = 2.07 ± 0.12. When the fractal dimension $D \approx 2$, the fractal model predicts that the closed time histogram is a power law and thus a straight line on such a log-log plot. The lines are the best fit of such a power law to the data.

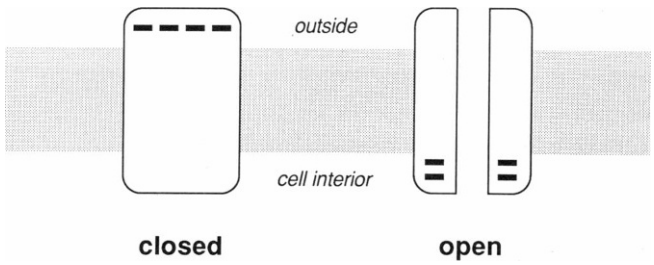


FIGURE 11. When the ion channel opens or closes there is a net movement of charge across the channel protein. Based on the voltage dependence the fractal model suggests that approximately one net negative charge moves inward when the channel opens and one net negative charge moves outward when the channel closes.

that, as shown in Fig. 11, there is a net movement of negative charge inward when the channel opens and an identical movement of net negative charge outward when the channel closes. If the voltage simply adds to the existing energy barriers then the kinetic setpoints will have the form $A = A_0 e^{zeV/kT}$ where $A_0$ is a constant, $z$ the net gating charge, $e$ the charge on an ion, $V$ the voltage, $k$ the Boltzmann constant, and $T$ the absolute temperature. From that relationship and the slope of the plots of $\log[A]$ vs. voltage we estimate that 0.53 ± 0.06 net negative charges move inward when the channel opens and that 0.74 ± 0.01 net negative charges move outward when the channel closes. Considering both the possible systematic and random errors involved in this determination, the near equality of these two numbers is important. The number of gating charges calculated from the data depends on the analysis used. Thus, unlike the Markov model, the fractal analysis leads to a consistent number of gating charges for both opening and closing, which provides strong support for the fractal interpretation of ion channel kinetics.

The variation of the time constants of the multiexponential fits to the frequency histograms of the closed and open times and the kinetic rate constants of the Markov model suggest no physical interpretation of the voltage dependence. On the other hand, the variation of $A$ and $D$ of the fractal model described above leads to a clear, simple, physical interpretation of the voltage dependence; namely, that the energy to open or close the channel $\Delta E = (\Delta E)_0 + (\Delta E)_g$, where $(\Delta E)_0$ is the intrinsic energy difference between the open and closed conformation of the channel and $(\Delta E)_g$ is the energy required to move the gating charges through the voltage applied across the patch. This simple model explains the variation of $\log[A]$ vs. voltage and thus the voltage dependence of all the short, medium, and long closed and open times of the channel.

Moreover, as shown above when $D \approx 2$, the probability density of the open or closed times has the form $f(t) \approx A\exp\{-[A/(2-D)]\}t^{1-D-A}$. For this $K^+$ channel we found that the fractal dimension $D$ does not vary with voltage while the kinetic setpoint $A$ does indeed depend on the voltage. For any channel with a similar form for the voltage dependence of $D$ and $A$, when $D \approx 2$ the exponential term will be exquisitely sensitive to small changes in $A$. Hence, when $D \approx 2$ small changes in the voltage-dependent kinetic setpoint $A$ will dramatically change the open or closed time distribution. Thus, if the fractal model is correct, then the fractal dimension measured at a single voltage can be used to predict the voltage sensitivity of an ion channel. For the $K^+$ channel we observed, $D$(closed) ≈ 2 and so the voltage dependence of $A$(closed) greatly increases the probability of the channel remaining closed for long durations as the patch is hyperpolarized, effectively turning the channel off.

The frequency histograms of the open and closed durations of many ion channels have been quite successfully fit by multiple state Markov models (1, 2). Does this extensive literature contradict the fractal model? It is too early to tell. The extant data will have to be re-analyzed from the fractal viewpoint and the fractal and Markov models compared. This will require the original data, because it is almost impossible to do from the published results. Nonetheless, some of the published results are quite suggestive. For example, Blatz and Magleby (76) found that the distribution of closed times of a chloride channel is overall a power law, which to us suggests that the kinetics is fractal with fractal dimension ≈2. The small scale features of this data could be interpreted either as (*a*) a fractal continuum of states, separated by small energy barriers, some of which are longer lived than others, or (*b*) as due to the sum of discrete Markov states separated by steep energy barriers. The resolution of this issue will depend on future biophysical measurements of ion channel protein dynamics. Qualitatively, a stretched exponential form, characteristic of fractals, is the form most often seen for the distribution of open and closed times in published single channel papers. Nonetheless, qualitative judgments are not conclusive. The data must be rigorously re-analyzed to determine if it is consistent with or contradicts the fractal model.

The two channels that we have analyzed, the $K^+$ channel in an excitable cell presented here and a nonselective channel in an epithelium (24–26), are well fit by the fractal model. If the fractal model applies to other channels as well then the fractal dimension $D$ and the kinetic setpoint $A$ may serve as a useful phenomenological classification scheme of ion channel types. If that is true, then we will be faced with the entertaining challenge of trying to derive $D$ and $A$ from ion channel structure and dynamics.

We thank Dr. Fred Sachs for the opportunity for one of us (J. M. Sullivan) to visit his laboratory and Anthony Auerbach and Jim Neal for their assistance in using the patch clamp and Markov analysis software developed in that laboratory. J. M. Sullivan also thanks his Ph.D. thesis committee and specifically Dr. Stephen Cohen for the use of his laboratory facilities and the aid of his technical personnel who provided cultured hippocampal cells. We also thank Ms. Mei Wang who assisted in this work and measured 1,551 closed and 1,551 open durations from the chart recordings. The development of the fractal model of ion channel kinetics has benefited from helpful discussions with Leo Levine, Michael Shlesinger, Howard Eggers, Raúl Chiesa, Lu-Ku Li, Stefan Machlup, Jorge Fischbarg, and Jan Koniarek. Healthy and helpful criticisms were also provided by Watt Webb, Fred Sachs, and Karl Magleby.

This work was supported in part by National Institutes of Health grants EY6234, EY1080, EY6178, GM7280, and NIDA3613.

*Received for publication 5 June 1987 and in final form 5 August 1987.*

## REFERENCES

1. Sakmann, B., and E. Neher, editors. 1983. Single Channel Recording. Plenum Publishing Corp., New York.
2. Hille, B. 1984. Ionic Channels of Excitable Membranes. Sinauer Associates Inc., Sunderland, MA.
3. Stevens, C. 1972. Inferences about membrane noise from electrical measurements. *Biophys. J.* 12:1028–1047.
4. Verveen, A. A., and L. J. DeFelice. 1974. Membrane noise. *Prog. Biophys.* 28:189–265.

5. Conti, F., and E. Wanke. 1975. Channel noise in nerve membranes and lipid bilayers. *Q. Rev. Biophys.* 8:451–506.
6. van Driessche, W., and K. G. Gullentops. 1978. Conductance fluctuation analysis in epithelia. *Tech. Cell Physiol.* P123:1–13.
7. Lindemann, B. 1980. The beginning of fluctuation analysis of epithelial ion transport. *J. Membr. Biol.* 54:1–11.
8. DeFelice, L. J. 1981. Introduction to Membrane Noise. Plenum Publishing Corp., New York.
9. Hamill, O. P., A. Marty, E. Neher, B. Sakmann, and F. J. Sigworth. 1980. Improved patch-clamp techniques for high-resolution current recording from cells and cell-free membrane patches. *Pflueg-ers Arch. Eur. J. Physiol.* 391:85–100.
10. Colquhoun, D., and A. G. Hawkes. 1977. Relaxation and fluctuations of membrane currents that flow through drug-operated channels. *Proc. R. Soc. Lond. B. Biol. Sci.* 199:231–262.
11. Colquhoun, D., and A. G. Hawkes. 1981. On the stochastic properties of single ion channels. *Proc. R. Soc. Lond. B. Biol. Sci.* 211:205–235.
12. Colquhoun, D., and A. G. Hawkes. 1982. On the stochastic properties of single ion channel openings and clusters of bursts. *Philos. Trans. R. Soc. Lond. B. Biol. Sci.* 300:1–59.
13. FitzHugh, R. 1983. Statistical properties of the asymmetric random telegraph signal, with applications to single-channel analysis. *Math. Biosci.* 64:75–89.
14. Jackson, M. B. 1985. Stochastic behavior of a many-channel membrane system. *Biophys. J.* 47:129–137.
15. Careri, G., P. Fasella, and E. Gratton. 1975. Statistical time events in enzymes: a physical assesment. *CRC Crit Rev. Biochem.* 3:141–164.
16. Gurd, F. R. N., and T. M. Rothgeb. 1979. Motions in proteins. *Adv. Prot. Chem.* 33:73–165.
17. Williams, R. J. P. 1979. The conformational properties of proteins in solution. *Bio. Rev.* 54:389–437.
18. Karplus, M., and J. A. McCammon. 1981. The internal dynamics of globular proteins. *CRC Crit. Rev. Biochem.* 9:293–349.
19. Karplus, M., and J. A. McCammon. 1983. Dynamics of proteins: elements and function. *Annu. Rev. Biochem.* 52:263–300.
20. Levitt, M. 1983. Molecular dynamics of native protein I. computer simulation of trajectories. *J. Mol. Biol.* 168:595–620.
21. Levitt, M. 1983. Molecular dynamics of native protein II. analysis and nature of motion. *J. Mol. Biol.* 168:621–657.
22. Ringe, D., and G. A. Petsko. 1985. Mapping protein dynamics by X-ray diffraction. *Prog. Biophys. Mol. Biol.* 45:197–235.
23. Karplus, M., and J. A. McCammon. 1986. The dynamics of proteins, *Sci. Am.* April 1986:42–51.
24. Liebovitch, L. S., J. Fischbarg, and J. P. Koniarek. 1986. Fractal model of ion channel kinetics. *J. Gen. Physiol.* 88:34a–35a. (Abstr.)
25. Liebovitch, L. S., J. Fischbarg, J. P. Koniarek, I. Todorova, and M. Wang. 1987. Fractal model of ion channel kinetics. *Biochim. Biophys. Acta.* 896:173–180.
26. Liebovitch, L. S., J. Fischbarg, and J. P. Koniarek. 1987. Ion channel kinetics: a model based on fractal scaling rather than multistate Markov processes. *Math. Biosci.* 84:37–68.
27. Wong, R. K. S., and R. B. Clark. 1983. Single $K^+$ channel currents from hippocampal pyramidal cells of adult guinea pig. *Soc. Neurosci. Abstr.* 9:602.
28. Sullivan, J. M., and S. A. Cohen. 1985. Single ion channels in cultured hippocampus show inward rectification. *Biophys. J.* 47:385a. (Abstr.)
29. Huguenard, J. R., and B. E. Alger. 1985. Properties of the inward rectifying potassium channel in acutely dissociated hippocampal pyramidal cells. *Soc. Neurosci. Abstr.* 11:786.
30. Sullivan, J. M. 1987. A voltage- and calcium-sensitive inward rectifying potassium channel active in the resting membrane of cultured mouse hippocampal neurons. *Biophys. J.* 51:54a. (Abstr.)
31. Sullivan, J. M. 1987. Patch clamp study of a large conductance, inward rectifying potassium channel in cultured mouse hippocampal neurons. Ph.D. Dissertation, City University, New York.
32. Mandelbrot, B. B. 1977. Fractals: Form, Chance, and Dimension. W. H. Freeman & Co. Publishers, San Francisco.
33. Mandelbrot, B. B. 1983. The Fractal Geometry of Nature. W. H. Freeman & Co. Publishers, San Francisco.
34. Barcellos, A. 1984. The fractal geometry of Mandelbrot. *College Math. J.* 15:98–114.
35. Gardner, M. 1976. In which "monster" curves force redefinition of the word "curve." *Sci. Am.* Dec. 1976:124–133.
36. Gardner, M. 1978. White and brown music, fractal curves and one-over-f fluctuations. *Sci. Am.* April 1978:16–32.
37. Gleick, J. 1985. The man who reshaped geometry. *N. Y. Times Sec. 6 (Mag.).* Dec. 5, 1985:64.
38. Anon. 1986. Mathematics with a twist. *Compressed Air Mag.* Aug. 1986:7–13.
39. Peitgen, H.-O., and P. H. Richter. 1986. The Beauty of Fractals. Springer-Verlag, New York.
40. Mandelbrot, B. B. 1967. How long is the coast of Britain? Statistical self-similarity and fractal dimension. *Science (Wash. DC).* 156:636–638.
41. Richardson, L. F. 1961. The problem of contiguity: an appendix to *Statistics of Deadly Quarrels. General Systems Yearbook.* 6:139–187.
42. Lovejoy, S. 1982. Area-perimeter relation for rain and cloud areas. *Science (Wash. DC).* 216:185–187.
43. Lewis, M., and D. C. Rees. 1985. Fractal surfaces of proteins. *Science (Wash. DC).* 230:1163–1165.
44. Avnir, D., D. Farin, and P. Pfeifer. 1984. Molecular fractal surfaces. *Nature (Lond.).* 308:261–263.
45. Paumgartner, D., G. Losa, and E. R. Weibel. 1981. Resolution effect on the sterological estimation of surface and volume and its interpretation in terms of fractal dimensions. *J. Microsc.* 121:51–63.
46. Lavenda, B. H. 1981. Brownian motion. *Sci. Am.* Feb. 1985:70–84.
47. Kagan, Y.Y., and L. Knopoff. 1981. Stochastic synthesis of earthquake catalogs. *J. Geophys. Res.* 86:2853–2862.
48. West, B., V. Bhargava, and A. L. Goldberger. 1986. Beyond the principle of similitude, renormalization in the bronchial tree. *J. Appl. Physiol.* 60:1089–1097.
49. Damme, H. V., F. Obrecht, P. Levitz, L. Gatineau, and C. Laroche. 1986. Fractal viscous fingering in clay slurries. *Nature (Lond.).* 320:731–733.
50. Stanley, H. E., and N. Ostrowksy, editors. 1986. On Growth and Form, Fractal and Non-Fractal Patterns in Physics. Martinus Nijhoff Publishers, Boston.
51. Miller A., W. Knoll, and H. Möhwald. 1986. Fractal and non-fractal crystalline phospholipid domains in monomolecular layers. *Biophys. J.* 49:317a. (Abstr.)
52. Ansari, A., J. Berendzen, S. F. Bowne, H. Frauenfelder, I. E. T. Iben, T. B. Sauke, E. Shyamsunder, and R. D. Young. 1985. Protein states and proteinquakes. *Proc. Natl. Acad. Sci. USA.* 82:5000–5004.
53. Sander, L. M. 1986. Fractal growth processes. *Nature (Lond.).* 322:789–793.
54. Orbach, R. 1986. Dynamics of fractal networks. *Science (Wash. DC).* 231:814–819.
55. Williams, G., and D. C. Watts. 1970. Non-symmetrical dielectric relaxation behavior arising from a simple empirical decay function. *Trans. Faraday Soc.* 66:80–85.
56. Shlesinger, M. F. 1984. Williams-Watts dielectric relaxation: a fractal time stochastic process. *J. Stat. Phys.* 36:639–648.
57. Klafter, J., and M. F. Shlesinger. 1986. On the relationship among the three theories of relaxation in disordered systems. *Proc. Natl. Acad. Sci. USA.* 83:848–851.
58. Cox, D. R. 1962. Renewal Theory. Science Paperbacks, London.

59. Peacock, J. H., D. F. Rush, and L. H. Mathers. 1979. Morphology of dissociated hippocampal cultures from fetal mice. *Brain Res.* 169:241–246.
60. Bornstein, M. B. 1958. Reconstituted rat tail collagen used as a substrate for tissue cultures in Maximov slides and roller tubes. *Lab. Invest.* 7:134–137.
61. Yavin, E., and Z. Yavin. 1974. Attachment and culture of dissociated cells from rat embryo cerebral hemispheres on polylysine-coated surface. *J. Cell Biol.* 62:540–546.
62. Letourneau, P. C. 1975. Possible roles for cell-to-substrate adhesion in neuronal morphogenesis. *Dev. Biol.* 44:77–91.
63. Bottenstein, J. E., and G. H. Sato. 1979. Growth of a rat neuroblastoma cell line in serum-free supplemented medium. *Proc. Natl. Acad. Sci. USA.* 76:514–517.
64. Bottenstein, J. E. 1983. Defined media for dissociated neural cultures. *In* Current Methods in Cellular Neurobiology. Volume IV. Model Systems. J. L. Barker and J. F. McKelvy, editors. John Wiley & Sons, Inc., New York. 107–127.
65. Seifert, W., B. Ranscht, H. J. Fink, F. Forster, S. Beckh, and W. H. Muller. 1983. Development of hippocampal neurons in cell culture: a molecular approach. *In* Neurobiology of the Hippocampus. W. Seifert, editor. Academic Press, Inc., New York. 7.
66. Corey, D. P., and C. F. Stevens. 1983. Science and technology of patch recording electrodes. *In* Single Channel Recording. B. Sakmann, and E. Neher, editors. Plenum Publishing Corp., New York. 53–68.
67. Fukushima, Y. 1981. Single channel potassium currents of the anomalous rectifier. *Nature (Lond.).* 294:368–371.
68. Fukushima, Y. 1982. Blocking kinetics of the anomalous potassium rectifier of tunicate egg studied by single channel recording. *J. Physiol. (Lond.).* 331:311–331.
69. Ohmori, H., S. Yoshida, and S. Hagiwara. 1981. Single $K^+$ channel currents of anomalous rectification in cultured rat myotubes. *Proc. Natl. Acad. Sci. USA.* 78:4960–4964.
70. Sakmann, B., and G. Trube. 1984. Voltage-dependent inactivation of inward rectifying single-channel currents in the guinea pig heart cell membrane. *J. Physiol. (Lond.).* 347:659–683.
71. Sachs, F., J. Neil, and N. Barkakati. 1982. The automated analysis of data from single ionic channels. *Pfluegers Arch. Eur. J. Physiol.* 395:331–340.
72. Auerbach, A., and F. Sachs. 1983. Flickering of a nicotinic ion channel to a subconductance state. *Biophys. J.* 42:1–10.
73. Auerbach, A., and F. Sachs. 1984. Single-channel currents from acetylcholine receptors in embryonic chick muscle: kinetic and conductance properties of gaps within bursts. *Biophys. J.* 45:187–918.
74. Press, W. H., B. P. Flannery, S. A. Teukolsky, and W. T. Vtterling. 1986. Numerical Recipes. Cambridge University Press, London.
75. Guharay, F., and F. Sachs. 1984. Stretch-activated single ion channel currents of tissue-cultured embryonic chick skeletal muscle. *J. Physiol. (Lond.).* 352:685–701.
76. Blatz, A. L., and K. L. Magleby. 1986. Quantitative description of three modes of activity of fast chloride channels from rat skeletal muscle. *J. Physiol. (Lond.).* 387:141–174.